Characterization of an Inductively Heated Plasma Generator and its Diagnostics

Kathryn Clements, Joshua Edgren, Michael Dropmann, René Laufer, Truell W. Hyde, and Lorin S. Matthews

***Abstract*—The IPG6-B is an inductively heated plasma generator located at Baylor University's Center for Astrophysics, Space Physics, and Engineering Research (CASPER) in Waco, Texas. Because the IPG6-B is relatively new, there remain many unknowns about its performance. During this project, a cavity calorimeter and a Pitot probe were used to characterize the facility by varying several operating parameters. Working gases included helium, argon, and nitrogen. The obtained data was used to calculate heat losses and Mach number of the plasma flow. Oscilloscope data of electric parameters was analyzed as well. Additionally, secondary effects, such as arcing and unstable discharges, were observed.**

***Index Terms*—Inductively Coupled Plasma, Plasma Diagnostics, Plasma Measurements, Plasma Properties**

I. Introduction

PLASMA is considered the fourth aggregate state [1]. It is defined as a partially ionized gas with roughly equal electron and ion density, making it quasi-neutral. It can be formed by heating a gas until its naturally occurring free electrons attain a kinetic energy greater than the ionization energy of the gas, thus creating more ions and electrons. Containing free electric charges, plasma has properties including electrical conductivity and the ability to be accelerated, contained, and heated by electric and magnetic fields [2].

The ability to produce plasma in the laboratory setting allows for the simulation of many plasma conditions of technical interest, for example those seen by spacecraft and fusion reactors. The way in which a spacecraft will charge in solar wind [3] and the performance of heat shield materials during atmospheric entry [4] are two aspects of spacecraft design which can be studied using lab-generated plasma.

Although there are multiple ways to create plasma, an inductively heated plasma generator (IPG) is advantageous in many respects. The main advantage of an IPG is that, unlike most other plasma generators, it does not use electrodes. Therefore, a large variety of gases can be used in an IPG, including chemically reactive gases that would erode the electrodes in other devices. This erosion not only causes damage to the equipment itself but also creates contaminates in the plasma that result in altered catalytic and radiative behavior [1]. Additionally, an IPG allows greater volumes of plasma to be studied at greater powers than a Gaseous Electronics Conference (GEC) cell [3] which only accommodates a small plasma volume. Lastly, an IPG can run for long periods of time allowing the study of steady state heat transfer whereas high-enthalpy shock tubes only offer a few milliseconds in which data can be taken [4].

The Center for Astrophysics, Space Physics, and Engineering Research (CASPER) at Baylor University in Waco, Texas is home to the IPG6-B. This facility is a modified version of the IPG6-S located at the Institute of Space Systems (IRS) at the University of Stuttgart in Germany. The heritage of both facilities can be traced to the IPG3, IPG4, and IPG5, all of which are from the IRS [3]. The objective of this project was to characterize the IPG6-B and its cavity calorimeter and Pitot probe by varying experimental parameters with the working gases helium, argon, and nitrogen.

II. Methods

The following section explains the IPG6-B facility and the working principles of the IPG and the diagnostics used, the cavity calorimeter and the Pitot probe.

A. Working Principle of the IPG

A high frequency (HF) current is fed into the copper coil surrounding the quartz tube of the IPG. This coil current results in a strong, oscillating magnetic field in the direction of the tube's centerline. The magnetic field in turn creates an azimuthal electric field within the tube. The naturally occurring free electrons in the gas are accelerated by the electric field. When the kinetic energies of these individual

Manuscript received August 7, 2015. This work was supported by the National Science Foundation Grant PHY-1262031.

K. Clements was with the Center for Astrophysics, Space Physics, and Engineering Research, Baylor University, Waco, TX 76798 USA. She is currently an undergraduate student at Saint Louis University, St. Louis, MO 63103 USA (e-mail: clementskate8@gmail.com).

J. Edgren was with the Center for Astrophysics, Space Physics, and Engineering Research, Baylor University, Waco, TX 76798 USA. He is currently an undergraduate student at Union University, Jackson, TN 38305 USA (e-mail: josh.edgren@gmail.com).

M. Dropmann is with the Center for Astrophysics, Space Physics and Engineering Research, Baylor University,Waco, TX 76798 USA. He is currently a doctoral student at the Univesity of Stuttgart, Stuttgart, Germany (email: michael_dropmann@baylor.edu).

R. Laufer, J. Schmoke, M. Cook, and T.W. Hyde are with the Center for Astrophysics, Space Physics and Engineering Research, Baylor University,Waco, TX 76798 USA (e-mail: rene_laufer@baylor.edu; truell_hyde@baylor.edu; jimmy_schmoke@baylor.edu; mike_cook@baylor.edu).

free electrons surpasses the ionization energy of the gas atoms, collisions between the atoms and free electrons ionizes the gas, turning it into plasma and freeing additional electrons leading to a chain reaction. The resulting free electrons and ions increase the electrical conductivity of the plasma leading to electrical current which heats the plasma. The operating principle can also be described by the transformer principle with the coil as a primary coil and the plasma acting as a secondary coil with only one turn [3]. A diagram of this process can be found in Fig. 1.

The current in the plasma always flows in the opposite direction of the current in the coil. Therefore, the magnetic field resulting from the current in the plasma is always in the opposite direction of the magnetic field caused by the current

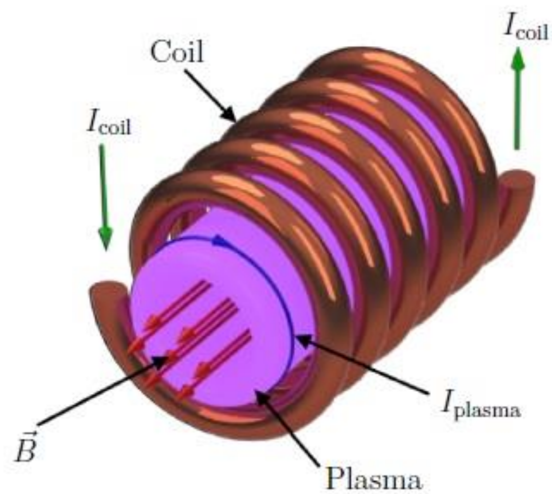

Fig. 1. IPG working principle [4]

in the coil. This fact leads to an important aspect of plasma behavior called the skin effect. The plasma's magnetic field damps that of the coil, most notably along the centerline. Because the area near the inner wall of the tube is least affected by the damping, the plasma is formed mostly in this region, and the plasma has a ring-shaped cross-section [5].

B. Facility Setup

A radio frequency (RF) generator provides the current to IPG coil. The power supply can provide a maximum of 15 kW of power and operates at a frequency of 13.56 MHz. It has an internal impedance is 50 Ω. The facility features a tuning network which is used to manually adjust the IPG's impedance so that it matches that of the power supply. This minimizes the reflected power and, thus, maximizes the efficiency [1].

The coil is made of copper tubing and has cooling water running through it. The coil is also cooled by the water flowing around the quartz tube. The tube is 40 mm in diameter and 1.5 mm thick. The coil tubing is 8 mm in diameter and has 5.5 turns. It is about 80 mm long. The whole IPG including its outer casing is about 230 mm long with a diameter of about 130 mm [3]. The IPG is housed in a Faraday cage to provide protection from the radio frequency (RF) field it emits [2].

One improvement of the IPG6-B over the IPG6-S is its injector design. With the new design, the shape of the plasma discharge can be observed from the back of the IPG via a mirror in the Faraday cage. Gas is injected into the IPG in such a way that it rotates making for a more stable plasma [3]. When the plasma leaves the quartz tube, it enters a large stainless steel vacuum chamber. The pressure in the chamber is regulated by a butterfly valve and a two stage pump. The chamber features guide rails and a sled on the inside. Diagnostics can be mounted to the universal probe holder on this sled [2].

C. Working Principle of the Cavity Calorimeter

The diagnostic used for most of this project was the cavity calorimeter. The cavity calorimeter is a copper cone with water-cooled tubing coiled mainly around the outside but also on the inside. The calorimeter's purpose is to absorb as much of the plasma's energy as possible so that the IPG's efficiency can be experimentally evaluated under differing conditions.

The plasma enters the calorimeter, and its energy is transferred to the inner tubing and wall in the form of heat. This heat is then transferred to the outer tubing as well. The inlet and exit temperatures of the cooling water are measured. Heat loss per unit time in the calorimeter can then be calculated using the volume flow rate and specific heat capacity of water. The recombined gas leaves the calorimeter with negligible kinetic and thermal energy making calorimeter heat loss an accurate measure of plasma power. The average specific enthalpy of the plasma can also be calculated [3].

D. Working Principle of the Pitot Probe

The Pitot probe is a diagnostic designed to measure total pressure. It consists of a water-cooled tube placed parallel to the plasma jet. The measured total pressure can be used to calculate the dynamic pressure and Mach number of the plasma jet [3].

III. Results

The following section presents the quantitative and qualitative findings corresponding to the gas used. LabView was used to collect data from a data logger and an oscilloscope. Data was recorded every 4 seconds analyzed using MATLAB. All experiments were run following warmups that incrementally increased the RF load power up to 5 kW. Experiments were then performed at 4 kW.

A. Helium

The helium plasma was magenta in color, and it became brighter at higher powers. It became redder at higher pressures and flow rates.

The helium data was analyzed to find some general trends. The calorimeter heat loss increased with pressure and increased slightly with flow rate. The IPG heat loss had a minimum at approximately 500 Pa, roughly in the middle of the pressures tested.

1) Sparking

One observed behavior in the helium plasma was sparking along the top rails inside the vacuum chamber. This occurred consistently at 300 and 400 Pa. The calorimeter was at a distance of 25 mm. The sparking did not appear to change with flow rate. This also occurred to a lesser extent during a few of the transitions to different vacuum pressures.

2) Arcing

Another observed behavior in the helium plasma was arcing. Arcing is caused by the potential difference between plasma and the walls of the vacuum chamber [2]. When arcing occurs, the chamber gets suddenly dark for a short time, because the arc, which is reminiscent of a lightning bolt, temporarily replaces the usual plasma jet. This is potentially damaging to the diagnostics, because the resistance of the plasma is greatly reduced resulting in a short circuit [2]. Melting often occurs where the arc attaches. In the data, arcing is most easily detected by sharp dips in the pressure.

There was very strong arcing at 1100 Pa which continued even after the power was turned down to 2 kW. Earlier in the experiment, singular less notable flickers were observed at 900 Pa and 1000 Pa. They were not observed directly enough to conclusively say whether they were arcs or just sparks, but the data indicates that they were small arcs.

3) Temperature Difference

The last unexpected aspect of behavior observed was that the plasma flow favored the upper part of the IPG. It appeared to flow slightly upward instead of straight out. It was forming more at the top of the quartz tube than at the bottom, and the top of the plasma jet was visibly brighter than the bottom. This was reflected in the data (shown in Fig. 2) by Sensor 2, located on the upper part of the IPG flange, reading significantly higher temperatures than Sensor 1, located on the lower part of the flange. The placement of the sensors is shown in Fig. 3. The temperature difference decreased with time, and eventually Sensor 1's reading would surpass that of Sensor 2. This temperature difference occurred with the other gases as well, but it was to a much lesser extent, and Sensor 2's reading was not always higher under these differing conditions.

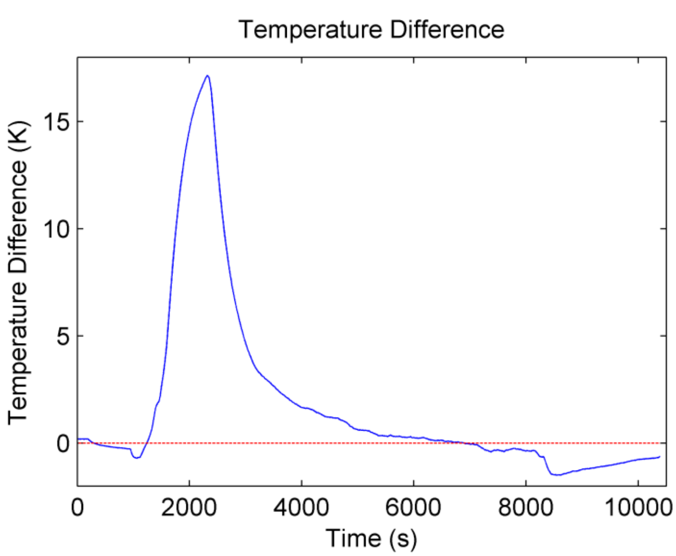

Fig. 3. Temperature difference between Sensor 2 and Sensor 1 as a function of time.

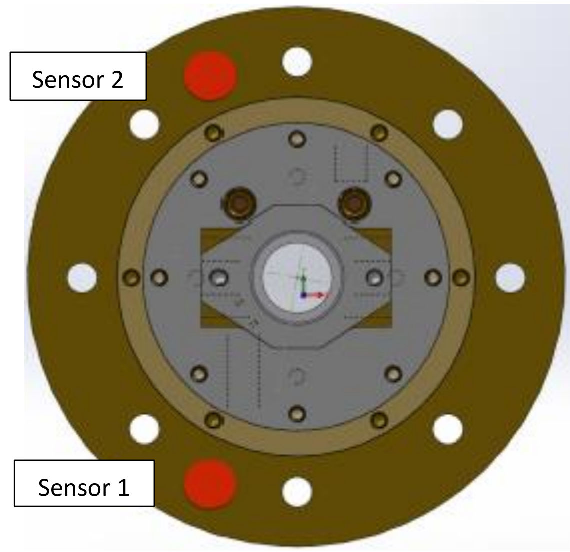

Fig. 2. Sensor placement on IPG flange.

B. Argon

The argon plasma was purple in color with a blue ring inside of the plume at the IPG exit. It became whiter at the higher power of 5 kW during warmup and once while reducing the pressure. There were several flashes observed during the warmup when performed at 100 Pa. The data indicates that these flashes were likely arcs. The warmup went more smoothly when performed at 200 Pa.

The pressure was unstable at 700 Pa. The pressure was increased to 1000 Pa, and it was unstable there, too. Both the IPG and calorimeter heat losses generally decreased with pressure.

1) Unstable, Rotating Discharges

An interesting phenomenon seen in the argon plasma was what looked like rotating strings of plasma pods. This pattern is shown in Fig. 4. When the warmup was conducted at 200 Pa, this was first noticed at a power of 1.5 kW. The behavior changed slightly at each pressure but persisted throughout the experiment.

When the calorimeter was moved to the back of the chamber so that it would be out of the way, a very rapid blinking light pattern was first noticed at 200 Pa and 4 kW. At 300 Pa it slowed down and rotated, looking much more like what was seen when the calorimeter was closer.

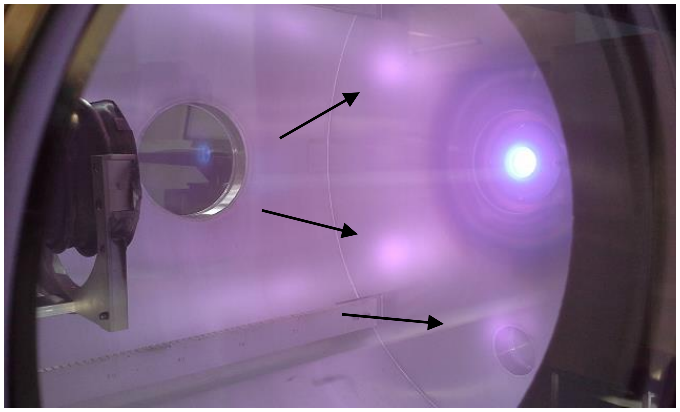

Fig. 4. Argon discharges.

2) IPG Heat Loss Fluctuations

During the argon experiments, there were significant fluctuations in the IPG heat loss, even when the power, pressure, and flow rate were stable. A code was written to quantify these fluctuations. It calculated the average IPG heat loss for each pressure and averaged each actual data point's deviation from that. The gas flow was constant for all data points considered in this analysis. The results of this analysis are shown in Fig. 5.

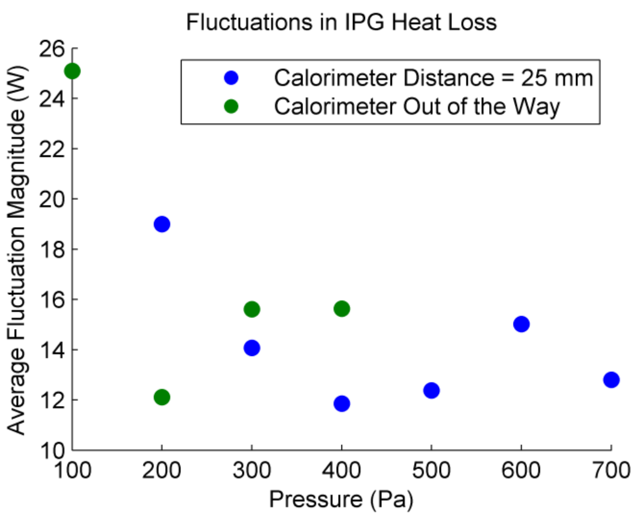

Fig. 5. Fluctuations in IPG heat loss at varying pressures.

C. Nitrogen

The nitrogen plasma was typically orange-yellow, although it became pink at higher pressures and gas flow rates. There was often an illuminated circle around the IPG exit. It was purple and more clearly defined on the bottom than the top when using the calorimeter. The glow reflections in the chamber were brighter at lower pressures and appeared unaffected by flow rate. At higher pressures, there was very little reflection in the chamber which showed that the plasma does not expand much due to higher pressures in the chamber. For the runs involving a calorimeter, these observations suggest that the calorimeter was capturing most of the plasma at higher pressures. However, this trend still took place with the Pitot probe.

Trends related to heat loss differed from those observed with helium and argon. With nitrogen, the IPG heat loss decreased with increasing flow rate at a given pressure, and it increased with pressure at a given flow rate. The calorimeter heat loss increased with flow rate and was unaffected by pressure.

Despite mostly stable behavior there were some occasional brief flashes at 5 kW during warmups. There was one experiment in which there was flickering after completing the warmup, and the IPG was shut down. While warming it up again, an arc was observed from the IPG to the side of the calorimeter just past the third coil. The grounding strip was removed, and the experiment proceeded normally after that.

1) Oscilloscope

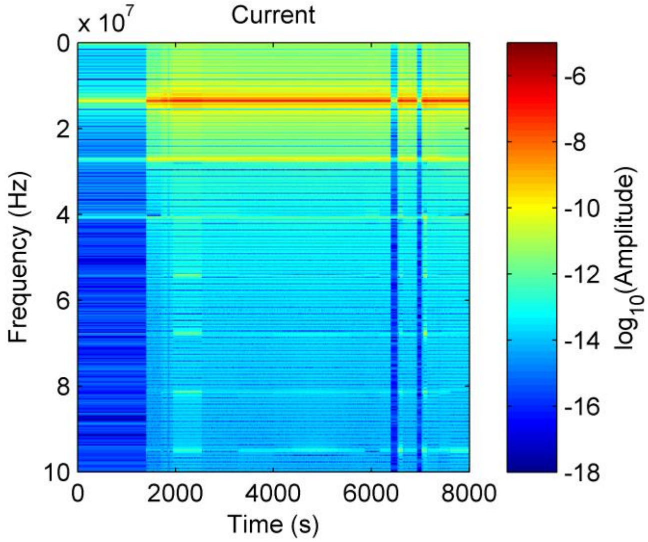

Fig. 10. Current data in frequency domain. The color scale is in arbitrary units.

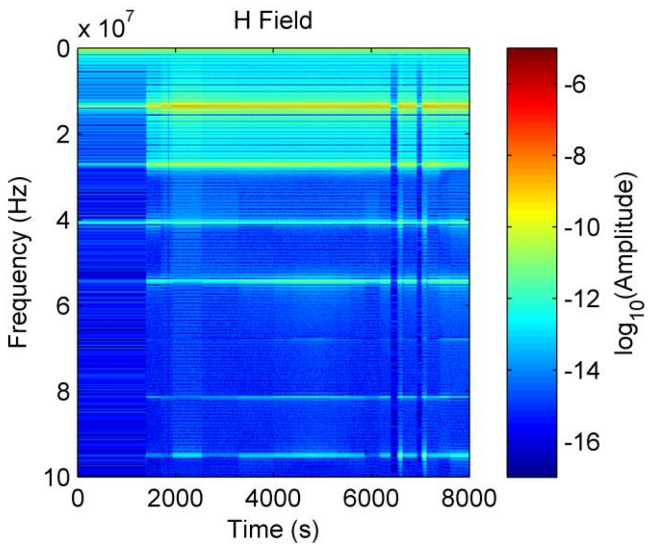

Fig. 8. H field data in frequency domain. The color scale is in arbitrary units.

Oscilloscope data was analyzed for one of the nitrogen experiments. Three channels were utilized to measure current, electric field (E field), and magnetic field (H field). A Fourier analysis was performed. The plots in Fig. 6, Fig. 8, and Fig. 9 show the results of this analysis. As expected, the highest magnitudes were at the operating frequency. Local maximums at some of its harmonics were visible, as well. Additionally, the faint but defined vertical bands in the images indicate that the amplitudes changed slightly with changes in the experimental parameters. The darker vertical bands indicate time intervals when the power supply was turned off.

The oscilloscope data also made it possible to find the phase differences between current, E field, and H field. The phase difference between the E field and H field was of particular interest. Fig. 10 shows how this phase difference changed with time. The fact that the phase difference is always positive indicates that the H field led the E field for the duration of the experiment. This result was expected, because the IPG is

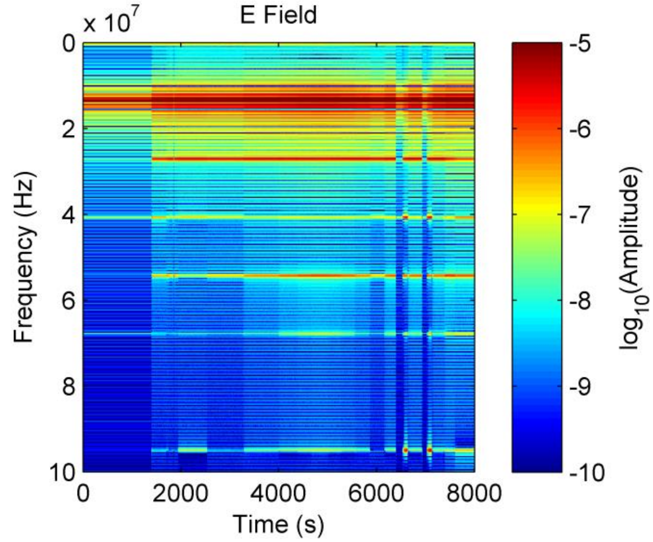

Fig. 9. E field data in frequency domain. The color scale is in arbitrary units.

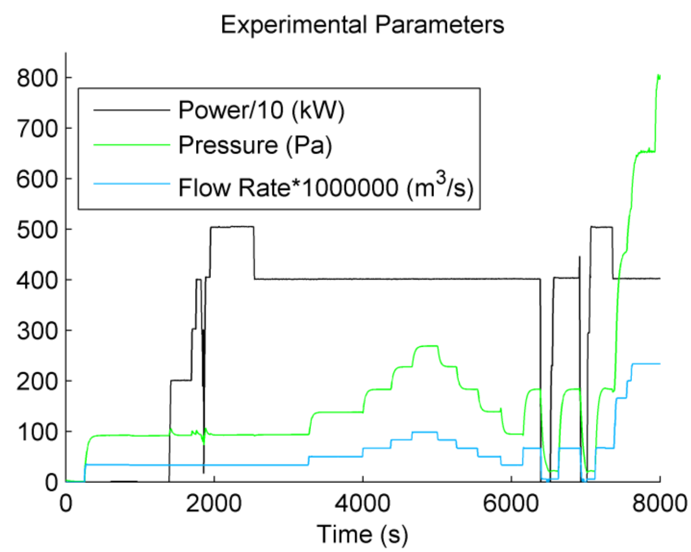

Fig. 7. Experimental parameters corresponding to Fig. 5

primarily an inductor. Fig. 10 can be compared with Fig. 12 to see how the changes in pressure, flow rate, and power affected the phase difference. The phase difference increased with

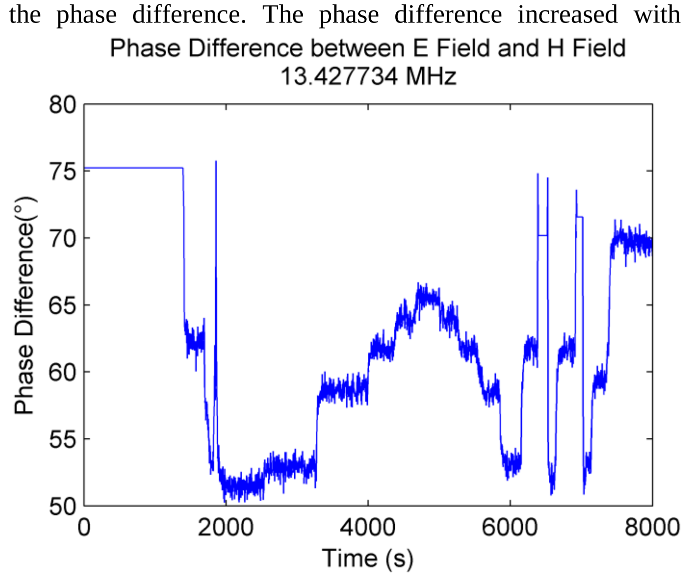

Fig. 6. Phase difference between E field and H field at frequency closest to operating frequency of 13.56 MHz. The phase angle of the E field was subtracted from that of the H field.

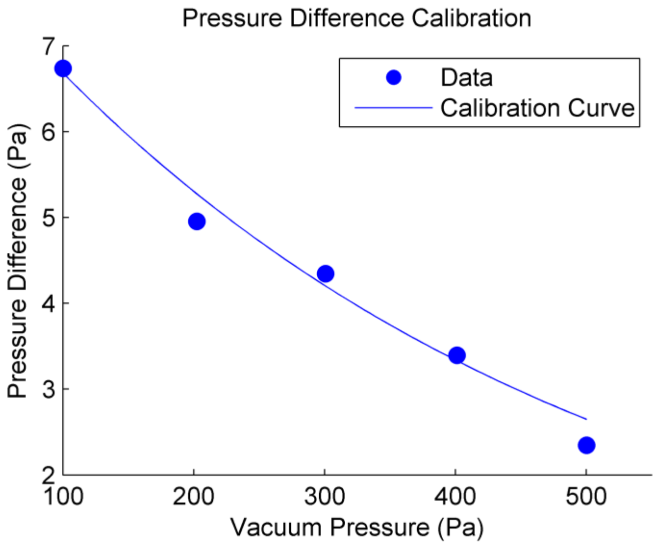

Fig. 11. Data and calibration curve used to calibrate Pitot probe.

increases in pressure and flow rate. The phase difference decreased with increases in power. The maximum phase difference for the main part of the experiment was about 66° which occurred at approximately 269 Pa and 9.849*10^{-7} m^3/s. An additional trend to note is that the greater the pressure and flow rate, the smaller the jump or drop in the phase difference was.

2) Pitot Probe

Because this was the first time using the Pitot probe, it needed to be calibrated. Data was taken at different pressures with the power and gas flow turned off. Under these conditions, the total pressure measured by the Pitot probe should have matched the vacuum pressure. The significant difference between the vacuum pressure and the uncalibrated Pitot pressure necessitated calibration. Using the difference between the measured and expected pressures, the MATLAB code was altered to correct this discrepancy. Fig. 14 shows the data and calibration curve for the pressure difference. The calibration equation is given in (1). Calibrated Pitot pressure is

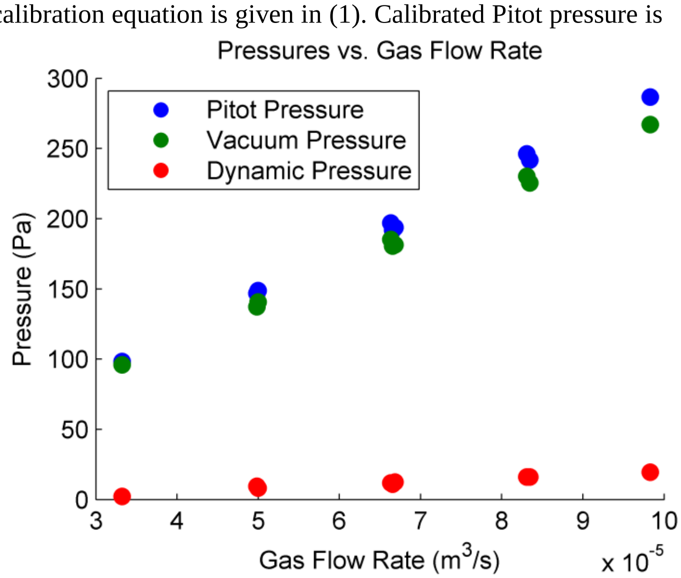

Fig. 13. Pressures as a function of gas flow rate. The butterfly valve was open for the entirety of this experiment.

p_{cal}, and measured Pitot pressure is p_{meas}.

$$\mathrm{p_{cal}} = \mathrm{p_{meas}} - 8.424exp(-0.002314\mathrm{p_{meas}}) \tag{1}$$

The calibrated pressure data (shown in Fig. 11) was then employed to calculate Mach number using (2) from [5]. *Ma* is the Mach number, γ is the adiabatic coefficient which is equal to 1.4 for nitrogen, p_{Pitot} is the Pitot pressure, and p_{vac} is the vacuum. The results are shown in Fig. 13. The Mach number increases with flow rate and decreases with vacuum pressure. Even the highest Mach number shown for this experiment is only about 0.32, indicating that the plasma was well within the subsonic region. This confirms that (2) is the appropriate equation to be using.

$$Ma = \sqrt{\frac{2}{\gamma-1}\left[\left(\frac{p_{Pitot}}{p_{vac}}\right)^{\frac{\gamma-1}{\gamma}} - 1\right]} \tag{2}$$

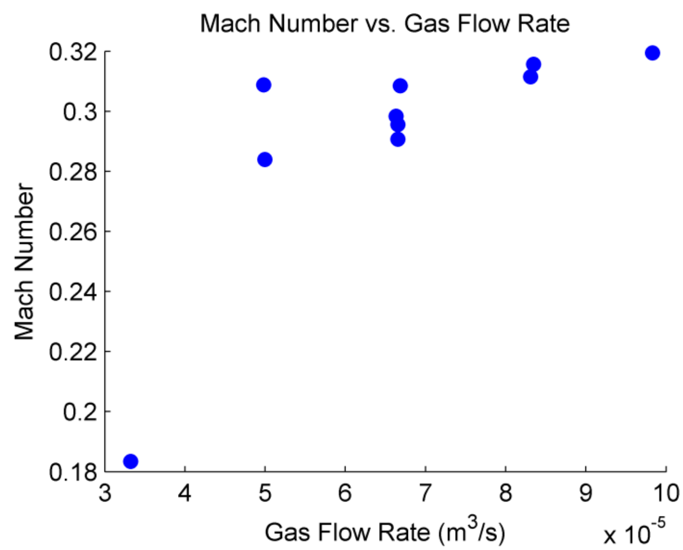

Fig. 12. Mach number as a function of gas flow rate.

IV. Discussion

It is unclear what the cause of the temperature difference in the IPG flange for argon is. Possible causes include electrical effects and calorimeter influence. A convective cause was ruled out, because the lower part of the flange was warmer than the upper part under some conditions

The unusual discharge pattern seen in the argon is due to its conductivity. The "pods" do not actually move. They are actually regions of glowing alternating with regions of non-glowing. The electric field throughout the plasma jet accelerates the plasma until it can ionize. Photons are released upon recombination. It stops glowing after this release and accelerates again. This behavior is thought to be due to argons high conductivity and the capacitive mode the IPG was suspected to be in.

The oscilloscope data analysis was important, because it revealed distinct changes in the impedance of the plasma generator. This knowledge can helpful for determining the transition from the capacitive mode to the inductive mode. It is advantageous to operate in the inductive mode, because the inductive mode is more efficient than the capacitive mode [4]. In the future, the MATLAB code used for this analysis will be run for other gases to analyze their modes and behaviors from this perspective. Another interesting application of the code would be to run it for an experiment in which the pressure and flow rate were varied separately. It could not be determined from the experiment analyzed in this paper whether pressure or flow rate had the greater influence on the phase difference, because the pressure and flow rate changed simultaneously due to the butterfly valve being kept open.

V. Conclusion

This project examined the behavior of the IPG and the plasma produced under varying conditions such as vacuum pressure, gas flow rate, and RF load power. This behavior was compared for helium, argon, and nitrogen. Additionally, observed phenomena such as arcing and unstable, rotating discharges were described and examined. Data oddities such as temperature differences across the IPG flange and IPG heat loss fluctuations were also described and analyzed.

Despite all of the knowledge gained from this project, there still remain unanswered questions. Further experimentation and analyses are planned beyond what time allowed for the purposes of this paper.

Acknowledgment

Kathryn Clements would like to thank Joshua Edgren for his collaboration and Michael Dropmann for his guidance throughout the project. She would additionally like to thank Jimmy Schmoke and Mike Cook for their assistance with the lab equipment as well as Dr. Truell Hyde and Dr. Lorin Matthews for their support and for making the REU program what it is. She would like to thank Sherri Honza for her logistical coordination. Finally, she would like to thank CASPER and the National Science Foundation for providing this opportunity. This work was supported by NSF grant No. PHY-1262031.

References

[1] Boehm, Kirk, "Characterization of the Inductively Heated Plasma Source IPG6-B using Helium," Diplom thesis, Technical University of Dresden, 2015.

[2] Schuff, Matthias, "Development of Measurement Inserts for a Multipurpose Plasma Diagnostic Probe," Research thesis, University of Stuttgart, 2015.

[3] M. Dropmann, G. Herdrich, R. Laufer, D. Puckert, H. Fulge, S. Fasoulas, J. Schmoke, M. Cook, and T. W. Hyde, "A New Inductively Driven Plasma Generator (IPG6)—Setup and Initial Experiments," *IEEE Trans. Plasma Sci.*, vol. 41, no. 4, pp. 804–810, Apr. 2013.

[4] Nikolai Sterionow, "Development of an Advanced Heat Flux Probe for High Enthalpy Plasma Flows," Diplom thesis, University of Stuttgart, 2014.

[5] G. Herdrich and D. Petkow, "High-enthalpy, water-cooled and thin-walled ICP sources characterization and MHD optimization," *J. Plasma Phys.*, vol. 74, no. 03, pp. 391–429, Jun. 2008.

Kathryn Clements was born in Glens Falls, NY in 1995. She will receive the B.S. degree in aerospace engineering from Saint Louis University, St. Louis, MO in 2017.

She is currently an Engineer at Saint Louis University's Space Systems Research Lab, St. Louis, MO. Ms. Clements is a member of the Society of Women Engineers. She was a recipient of the Excellence in Mathematics Award (Department of Mathematics and Computer Science, Saint Louis University) in 2014.

Joshua Edgren is a student at Union University in Jackson, TN and will receive his B.S. in physics in 2016. He is a member of the Society of Physics Students (SPS) and a part of the Research Experience for Undergraduates program at Baylor University's Center for Astrophysics, Space Physics, and Engineering Research (CASPER). He received the Kyle L. Hathcox Memorial Physics award in 2015 (Union University), and his research interests include plasma facilities, plasma conductivity, and space sciences.

Michael Dropmann received the diploma in aerospace engineering from the University of Stuttgart, Stuttgart, Germany, where he is currently working toward the Ph.D. degree in the Institute of Space Systems.

He is a Research Assistant with the Center for Astrophysics, Space Physics and Engineering Research (CASPER) and a member of the Space Science Lab of CASPER. His research interests include plasma facility design, plasma surface interactions, and space sciences.

René Laufer was born in Berlin, Germany, in 1968. He received the diploma in aerospace engineering from the Technical University of Berlin, Berlin, Germany and the Ph.D. degree from the University of Stuttgart, Stuttgart, Germany.

He is an Associate Research Professor with the Center for Astrophysics, Space Physics, and Engineering Research (CASPER) and the Head of the Space Science Lab of CASPER. He was involved in planetary missions at the DLR-Institute of Space Sensor Technology and Planetary Exploration and later became a Small-Satellite Project Manager and a Lecturer at the Institute of Space Systems, University of Stuttgart. His research interests include small satellites, lunar and planetary exploration, lunar bases, ISRU, dust and plasma, small bodies, remote sensing, systems engineering, education, and public outreach.

Truell W. Hyde was born in Lubbock, TX, in 1956. He received the B.S. degree in physics and mathematics from Southern Nazarene University, Bethany, OK, in 1978 and the Ph.D. degree in theoretical physics from Baylor University, Waco, TX, in 1988.

He is currently with Baylor University, where he is the Director of the Center for Astrophysics, Space Physics, and Engineering Research, a Professor of physics, and the Vice Provost for Research for the university. His research interests include space physics, shock physics and waves, and nonlinear phenomena in complex (dusty) plasmas.

Lorin S. Matthews was born in Paris, TX in 1972. She received the B.S. and the Ph.D. degrees in physics from Baylor University in Waco, TX, in 1994 and 1998, respectively.

She is currently an Assistant Professor in the Physics Department at Baylor University. Previously, she worked at Raytheon Aircraft Integration Systems where she was the Lead Vibroacoustics Engineer on NASA's SOFIA (Stratospheric Observatory for Infrared Astronomy) project.